Enzymatic generation of short chain cello-oligosaccharides from Miscanthus using different pretreatments

Kendrick, Emanuele G.; Bhatia, Rakesh; Barbosa, Fernando C.; Goldbeck, Rosana; Gallagher, Joe A.; Leak, David J.

Published in:
Bioresource Technology

DOI:
10.1016/j.biortech.2022.127399

Publication date:
2022

Citation for published version (APA):
Kendrick, E. G., Bhatia, R., Barbosa, F. C., Goldbeck, R., Gallagher, J. A., & Leak, D. J. (2022). Enzymatic generation of short chain cello-oligosaccharides from Miscanthus using different pretreatments. *Bioresource Technology*, *358*, [127399]. https://doi.org/10.1016/j.biortech.2022.127399

Bioresource Technology 358 (2022) 127399

Contents lists available at ScienceDirect

Bioresource Technology

journal homepage: www.elsevier.com/locate/biortech

Enzymatic generation of short chain cello-oligosaccharides from *Miscanthus* using different pretreatments

Emanuele G. Kendrick [a], Rakesh Bhatia [b,d], Fernando C. Barbosa [c], Rosana Goldbeck [c], Joe A. Gallagher [b], David J. Leak [a,*]

[a] Department of Biology & Biochemistry, University of Bath, Bath BA2 7AY, UK
[b] Institute of Biological, Environmental and Rural Sciences (IBERS), Aberystwyth University, Plas Gogerddan, Aberystwyth SY23 3EE, UK
[c] Bioprocess and Metabolic Engineering Laboratory, School of Food Engineering, University of Campinas (UNICAMP), Campinas, SP, Brazil
[d] Department of Agronomy and Plant Breeding, Justus Liebig University Giessen, Heinrich-Buff-Ring 26-32, 35392 Giessen, Germany

HIGHLIGHTS

- Recombinant enzyme-mediated COS (DP2-5) production from *Miscanthus Mx2779*.
- Optimised COS producing cellulolytic cocktail (TfCel9a, CcCel9m, OsCelC7 (−105)).
- COS yields from crystalline cellulose are limited by degradation into glucose.
- COS yields and DP profile are improved with swollen and amorphous cellulose.
- ~90 % conversion of glucan to COS (DP2-5) from [C_2mim][OAc] pretreated *Miscanthus*.

GRAPHICAL ABSTRACT

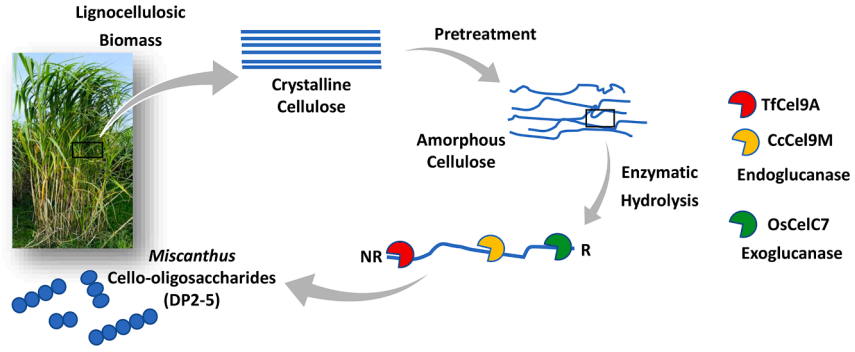

ARTICLE INFO

Keywords:
Cello-oligosaccharides
Miscanthus
Pretreatment
Cellulose
Enzymatic hydrolysis
Endoglucanases
Lytic polysaccharide monooxygenase

ABSTRACT

Enzyme combinations producing short-chain cello-oligosaccharides (COS) as major bio-products from cellulose of *Miscanthus Mx2779* accessed through different pretreatment methods were compared. Over short hydrolysis times, processive endoglucanase TfCel9a produced a high percentage of cellotetraose and cellopentaose and is synergistic with endoglucanase CcCel9m for producing short oligomers from amorphous cellulose but had low activity on untreated *Miscanthus*. Hydrolysis of the latter improved when these were combined with a mutant cellobio/triohydrolase OsCelC7(−105) and a lytic polysaccharide monooxygenase TrCel61a, a combination which also produced the highest COS yields from phosphoric acid swollen cellulose. Steam explosion pretreatment of *Miscanthus* increased COS yields, with/without phosphoric acid swelling, while increased swelling time (from 20 to 45 min) also increased yields but decreased the need for TrCel61a. The highest COS yields (933 mg/g glucan) and most stable product profile were obtained using ionic liquid [C_2mim][OAc] pretreatment and the three enzyme mixture TfCel9a, Cel9m and OsCel7a(−105).

* Corresponding author.
E-mail address: d.j.leak@bath.ac.uk (D.J. Leak).

https://doi.org/10.1016/j.biortech.2022.127399
Received 20 April 2022; Received in revised form 26 May 2022; Accepted 27 May 2022
Available online 29 May 2022

1. Introduction

Lignocellulose, including agricultural crop residues, woody and herbaceous biomass, represents the most abundant, renewable biological resource on Earth that is mainly exploited in the non-food sector, since it comprises the majority of inedible plant material. The utilisation of lignocellulose has garnered appeal as a potential supply of renewable energy (liquid, solid and gaseous biofuels) as well as materials and high value-added chemicals to ease the growing issues of global energy demand, sustainability and climate action. One of the major components of lignocellulose, cellulose, consists largely of crystalline β −1,4 linked glucan chains that can be enzymatically hydrolysed into its constituent glucose monomers and fermented microbially to produce bioethanol amongst other added-value compounds (Sanderson, 2011).

To expand the product range beyond bioethanol, cello-oligosaccharides (COS), linear oligomers of β-1,4 linked glucose residues, could also potentially be derived from the cellulose of lignocellulosic materials, and these have attracted attention as higher-value products for the pharmaceutical, chemical, food and feed industries (Ávila et al., 2021). Water soluble COS up to a degree of polymerisation (DP) of 6 glucose units fall into the category of non-digestible oligosaccharides (NDOs) that are fermentable by a number of gut microbiota including various *Lactobacillus* and *Bifidobacterium* species (Karnaouri et al., 2019; Jiao et al., 2014; Roberfroid and Slavin, 2000). As such they have been explored as potential prebiotic compounds that can be added to enrich dietary products and animal feed to support gastrointestinal health and function (Otsuka et al., 2004).

In addition, a promising application for COS as a novel substrate in fermentation is emerging, as an alternative to the conventional process utilising glucose (Barbosa et al., 2020). Direct fermentation of low DP (2–5) COS, without extracellular conversion to glucose, offers solutions to some of the key challenges in industrial bioethanol fermentation, particularly in the reduction of enzymatic processing and minimisation of process contamination. The scale of operations in industrial bioethanol production is prohibitive to heat-sterilisation, without which, yeast fermentations of glucose-rich substrates are prone to contamination by wild yeasts and other ethanol-tolerant species, impacting productivity (Basílio et al., 2008). The spectrum of species capable of metabolising COS in an ethanolic environment is relatively small, meaning that a monoculture during fermentation could be maintained when combining a COS–based substrate with an engineered species able to utilise them (Parisutham et al., 2017). The direct fermentation of COS also circumvents several other issues related to glucose fermentation including, i) the requirement for β-glucosidase supplementation during enzymatic saccharification to obtain glucose, which increases process cost; ii) the inhibition of co-utilisation of different sugars in the hydrolysate through catabolite repression; and iii) the inhibitory effects of glucose on other auxiliary saccharification enzymes, such as endoglucanases, which has presented a challenge for both separate hydrolysis (SHF) and simultaneous saccharification and fermentation (SSF) strategies (Borges et al., 2014; Hsieh et al., 2014; Parisutham et al., 2017). To this end, numerous different approaches have been implemented to engineer *S. cerevisiae* to ferment COS (Galazka et al., 2010; Hu et al., 2016; Kim et al., 2018; Parisutham et al., 2017).

During conventional cellulose hydrolysis with most commercial enzyme preparations, COS only exist as transitory intermediates. Nevertheless, through modification of commercial enzyme cocktails to reduce β-glucosidase activity, including chromatographic fractionation and the addition of inhibitors, as well as splitting the standard single-step hydrolysis reaction into multiple stages, COS recovery has been demonstrated (Chu et al., 2014; Karnaouri et al., 2019). However, typically these still generate a significant glucose fraction and currently the only COS that can be produced in significant quantities via this method is cellobiose (DP2). Non-enzymatic methods have been employed, to generate COS with a wider DP range. However, these methods require the use of harsh chemicals, such as concentrated hydrochloric and sulphuric acid, or energy-intensive temperature and pressure extremes and have only been applied to pure micro-crystalline cellulose (Tolonen et al., 2015; Zhang and Lynd, 2003). This probably limits their commercial viability as part of a COS-based biorefinery.

Enzyme-catalysed hydrolysis of cellulose into COS of > DP2 with minimal further degradation to glucose during prolonged reactions is achievable by a variety of GH5, GH9 and GH45 endoglucanases (Belaich et al., 2002; Karlsson et al., 2002; Song et al., 2017). In addition to these classical endoglucanases, processive endoglucanases, named for their unusual ability to processively bind, cleave and release COS along cellulose chains in a similar fashion to exoglucanases have also been proposed as candidates for COS production (Wu and Wu, 2020; Zverlov et al., 2005). Even though this processivity permits a certain degree of activity on crystalline cellulose, processive endoglucanases, along with classical endoglucanases, display the greatest activity on amorphous regions of cellulose meaning that, in the absence of an *exo*-acting cellulolytic enzyme capable of producing COSs, conversion to amorphous cellulose is probably required as a prerequisite for a COS production process (Béguin and Aubert, 1994; Karnaouri et al., 2017). There have been some studies reporting the activity of these individual COS-producing enzymes on representative models of crystalline and amorphous cellulosic substrates, as well as their synergy with other cellulolytic enzymes (Henrissat et al., 1985; Karnaouri et al., 2017; Kostylev and Wilson, 2014; Yang et al., 2016; Zverlov et al., 2005). However, to the authors' knowledge, no comprehensive studies compare multiple COS-producing endoglucanases in combination with assistive enzymes on lignocellulose-derived crystalline and amorphous cellulose, to define a process for the production of a range of soluble COS.

In a previous study, a number of recombinant endoglucanases were expressed and analysed for their synergy with lytic polysaccharide monooxygenases (LPMO), cellobiose dehydrogenase (CDH) and different additives for the hydrolysis of hydrothermally pretreated sugarcane straw to produce COS. Following process optimization via Design of Experiments, only a low COS yield (60.49 mg of COS/g glucan) was achieved with minimal glucose formation, 87 % of which was comprised of cellopentaose (Barbosa et al., 2020). Here, a study is presented for the improvement of final yield and product range in enzymatic COS production through analysing the activity of established recombinant endoglucanases and assistive enzymes on amorphous and native cellulose. For this, lignocellulosic biomass from the dedicated bioenergy crop *Miscanthus,* a genus of the photosynthetic efficient C_4 grasses and a close relative to the bioethanol crops sugarcane (*Saccharum*) and maize (*Zea mays*), was subjected to commonly used individual or combined pretreatment methods (steam explosion, phosphoric acid, [C_2mim][OAc] ionic liquid) to access the cellulose for enzymatic hydrolysis with select endoglucanases and an LPMO, with the introduction of limited *exo*-acting enzyme activity through the addition of a cellobio/triohydrolase. A potential pretreatment and enzymatic process strategy for the utilisation of *Miscanthus* biomass for COS (DP 2–5) production in high yield is highlighted.

2. Materials and methods

2.1. Strains and biological materials

E.coli BioBlue (*recA1 endA1 gyrA96 thi-1 hsdR17*($r_k^- m_k^+$) *supE44 relA1 lac* [F' *proAB lacI*^{q}*Z*△*M15* Tn*10*(Tet^r)] was purchased from Bioline (UK) and used in the assembly and storage of plasmids in this study. Wild type *P. pastoris* NRRL 11,430 (Northern Regional Research Laboratories, Peoria, USA) was used as the host organism for all enzyme expression. Codon optimised gene sequences encoding cellulolytic enzymes (see supplementary material) were designed and synthesised by GeneArt (Thermo Fisher Scientific, UK). All PCR primers were purchased from Eurofins (UK) (see supplementary material). pPICZαB was purchased from Thermo Fisher Scientific (UK). The enzymes encoded by the gene

sequences used in this study are summarised in Table 1.

2.2. Plant material

The *Miscanthus* genotype *Mx2779*, also known as GNT-14, a novel rapidly multiplied seeded interspecies hybrid (*Miscanthus sinensis* × *M. sacchariflorus*) was selected from the 2013 *Miscanthus* breeding program in Aberystwyth. Above-ground biomass (leaves and stem) following senescence of *Mx2779* was harvested in the spring of 2019. The biomass material was hammer chipped into an average size of ~ 10 to 30 mm and dried at 45 °C per technical report NREL/TP-510–42621 (Sluiter et al., 2008) to a moisture content of ≤ 10 % before steam explosion pretreatment. A representative portion of the untreated *Mx2779* biomass was hammer milled, sieved to a particle size of 0.18–0.85 mm per technical report NREL/TP-510–42620 (Hames et al., 2008). The material was then stored in air-tight sealable bags before phosphoric acid and [C_2mim][OAc] pre-treatment. The composition of the biomass (see supplementary material) before and after different pretreatments was determined as previously described (Bhatia et al., 2020).

2.3. Media and growth methods

All media reagents were purchased either from Merck (Gillingham, UK) or Fisher Scientific (Loughborough, UK). LB medium (0.5 % (w/v) yeast extract, 1.0 % (w/v) tryptone, 1.0 % (w/v) NaCl) with 25 μg/ml zeocin was used for the selection and growth of *E. coli* strains containing pPICZαB plasmids. Cultures were grown overnight at 37 °C, 250 rpm. YPD medium (1 % (w/v) yeast extract, 2 % (w/v) tryptone, 2 % (w/v) glucose) was used for the growth and storage of *P. pastoris* strains, with the addition of 100 μg/ml zeocin for selection of strains containing pPICZαB plasmids. For the expression of recombinant genes in *P. pastoris*, initial growth was conducted in BMGY (1 % (w/v) yeast extract, 2 % (w/v) tryptone, 1.34 % (w/v) yeast nitrogen base, 4 × 10–5 % (w/v) biotin, 100 mM potassium phosphate pH 6.0, 1 % (v/v) glycerol). Induction of expression was conducted in BMMY (1 % (w/v) yeast extract, 2 % (w/v) tryptone, 1.34 % (w/v) yeast nitrogen base, 4 × 10^{-5} % (w/v) biotin, 100 mM potassium phosphate pH 6.0, 0.5 % (v/v) methanol) supplemented by 3 % (w/v) sorbitol and 1 % (w/v) casamino acids.

For expression trials, *P. pastoris* strains were cultured from colonies on YPD agar plates in 50 mL centrifuge tubes in BMGY at 30 °C, 200 rpm for ~ 16 h. Cells were then centrifuged at 4000 rpm for 5 min and resuspended in 50 mL BMMY + sorbitol + casamino acids in 250 mL baffled flasks and incubated at 28 °C, 200 rpm for 3 days. Methanol was added to cultures every 24 h to a final concentration of 0.5 % (v/v). Culture supernatant was harvested by centrifugation at 4000 rpm for 10 min. Supernatants were either stored at −80 °C or concentrated and buffer exchanged by pressure-driven ultrafiltration using a Vivacell 100 (Sartorius, Epsom, UK) prior to storage at −80 °C.

2.4. Pretreatments for the generation of amorphous/swollen cellulosic substrates

Regenerated amorphous cellulose (RAC) was generated from Avicel (Merck, Gillingham, UK) according to Zhang et al. (2006). Steam explosion pretreatment of *Miscanthus Mx2779* was carried as described by Bhatia et al. (2020). Phosphoric acid (H_3PO_4) pretreatment of *Miscanthus Mx2779* was carried out as described previously (Sathitsuksanoh et al., 2012; Zhu et al., 2009). Briefly, one gram of dried untreated or steam exploded (SE) pretreated *Miscanthus* biomass was mixed with 8 mL of 85 % (w/w) H_3PO_4 in 50 mL Falcon tubes and the mixed slurry was then incubated for 20 or 45 min at 50 °C in a water bath. The reaction was stopped by placing tubes in an ice-water bath, adding 20 mL of 95 % (v/v) ethanol and mixing the slurry to precipitate dissolved cellulose and hemicellulose. The slurry was centrifuged at 3000 rpm at room temperature for 10 min, the supernatant was discarded, and the pellet was re-suspended and washed in 40 mL of 95 % (v/v) ethanol. After the ethanol washes, the solid pellet was centrifuged and washed two more times with 40 mL of deionised water. The residual solid pellet was finally neutralised to pH 5–7 with 2 M sodium carbonate, dried at 45 °C and finally weighed.

1-ethyl-3-methylimidazolium acetate ([Emim][Ac]), also known as [C_2mim][OAc], was purchased from Sigma-Aldrich. [C_2mim][OAc] pretreatment of *Miscanthus Mx2779* was performed as described by Bhatia et al. (2021). Briefly, 300 mg of senesced *Miscanthus* biomass (3 % w/w biomass loading) was mixed with 9.7 g of [C_2mim][OAc] and incubated at 160 °C for 3 h without stirring in 90 mL pressure tubes (Ace Glass). The samples were then transferred to 50 mL centrifuge tubes with 35 mL of hot de-ionised water and vigorously vortexed. The pulp was recovered by centrifugation at 3500 rpm for 10 min then washed repeatedly with 35 mL of hot de-ionised water (at least 4 times), centrifuged and then finally dried and weighed as above. All cellulosic residues were stored in air-tight containers until used for compositional analysis and enzymatic hydrolysis experiments.

Table 1

Name	Organism	Major reported product(s)	Other products	Length/ aa	NCB! Accession	Signal sequence	Reference
Processive encloglucanases							
CtCe19R	*Clostridium therrnocellum* F7	Cellotetraose	Cellobiose, glucose	736	A1585346.1	*a*-mating factor	Zverlov et al. (2005)
TfCeI9A	*Thermobifida fusca*	Cellotetraose	Cellotriose, cellobiose, glucose	880	AAB42155.1	*a*-mating factor	Irwin et al. (1998)
Classic endoglucanases							
CcCeI9M	*Clostridium cellulolyticum* ATCC 35,319	Cellotetraose	Cellot riose, cellobiose	526	IAAG45160.1	*a*-mating factor	Belaich et al. (2002)
TrCe145a	*Trichoderma reesei*	Cellotetraose	Cellotriose, cellobiose, glucose	242	CAA83846.1	*a*-mating factor	Karlsson et al. (2002)
CaCel	*Cryptopygus antarcticus*	Cellobiose, Cellotriose, Cellotetraose	N/a	225	ACV50414.1	*a*-mating factor	Song et al. (2017)
Cellobiohydrolases							
OsCelC7(−105)	*Orpinomyces* sp. In *02*	Cellotriose, cellobiose	Glucose I	344	A1103053.1	*a*-mating factor	Chen et al. (2014)
LPMOs							
TrCel6la	*Trichoderma reesei*	N/a	N/a	344	CAA71999.1	Native	Tanghe et al. (2015)

2.5. Fourier-transform infrared spectroscopy (FTIR)

FTIR analysis of untreated and pretreated *Miscanthus* biomass was performed according to Bhatia et al. (2021) using ~ 2 mg of milled sample (<80 μm) and a Thermo Nicolet iS50 FTIR spectrometer. The Spectral range included was 4000–400 cm^{-1} with a resolution of 4 cm^{-1} and spectra were obtained using eight scans and corrected for a baseline. The peaks in the 890 to 1430 region associated with crystalline and amorphous cellulose abundance were used to investigate cellulose modifications of *Miscanthus* samples after pretreatment (Bhatia et al., 2021).

2.6. Molecular biology

To insert constructs into pPICZαB downstream of the *AOX1* promoter and in-frame with the α-mating factor for secretion by *P. pastoris*, pPICZαB was PCR amplified with the primers pPICZabb-F and pPICZabb-R (see Supplementary Material) to generate a linear backbone. Synthetic constructs including the coding sequences for genes encoding the mature endoglucanases and OsCelC7(−105) were PCR amplified with primers to generate Gibson assembly parts with 40 bp overhangs complementary to the 5′ and 3′ ends of the pPICZαB amplicon. Parts were then integrated into the pPICZαB amplicon via Gibson assembly (Gibson et al., 2009) and transformed into *E. coli* for storage. Integration of the correct sequence was confirmed by sequencing (Eurofins Genomics, Germany). The expression constructs were then linearised within the *AOX1* region by a single restriction digest with SacI (Thermo Fisher Scientific, UK), cleaned and concentrated by ethanol precipitation and transformed into *P. pastoris* NRRL 11430 by electroporation, using the protocol from the EasySelect™ *Pichia* Expression Kit (Thermo Fisher, UK).

The cloning of TrCel61a was based on Tanghe et al. (2015) where it was demonstrated that the secreted yield of TrCel61a in *P. pastoris* could be improved by retaining the native signal sequence of the enzyme rather than using the α-mating factor in pPICZα. In contrast to the other enzymes, in which the DNA sequences encoding their native signal peptides were identified via SignalP (Almagro Armenteros et al., 2019) and omitted from synthesis, the codon optimised coding sequence of TrCel61a including its native signal sequence was used. pPICZαB was linearised by a double restriction digest with Bsp119I and NotI to remove the α-mating factor and a PCR amplicon of TrCel61a with its signal sequence was integrated by Gibson assembly. The transformation of the resulting expression construct into *P. pastoris* then followed the same method as outlined for the endoglucanase constructs.

2.7. Optimisation of recombinant enzyme production

To select for *P. pastoris* strains secreting higher recombinant enzyme titres through integrating multiple copies of the target construct, post transformational vector amplification in liquid culture, as described by Aw and Polizzi (2016), was conducted for each strain. A protocol to rapidly screen and compare secreted yields of active protein was adapted from de Amorim Araújo et al. (2015). Colonies expressing different endoglucanases or OsCbh-105 isolated after PTVA were picked and inoculated onto minimal methanol (1.34 % (w/v) yeast nitrogen base, 4×10^{-5} % (w/v) biotin, 100 mM potassium phosphate pH 6.0, 0.5 % (v/v) methanol) agar plates containing 0.5 % (w/v) carboxymethyl cellulose (CMC). Plates were incubated for 72 h upside down with 150 μl 100 % methanol added to the inside of the plate lids every 24 h to maintain induction. Hydrolysis halos representing zones around colonies in which CMC had been hydrolysed by secreted enzymes were visualised by staining the plates with 0.2 % Congo Red solution for 15 min and washing with 1 M NaCl. Plates were imaged with a Syngene G: Box ChemiHR system (Syngene, UK) and halo circumferences were measured with ImageJ (Schneider et al., 2012) and used to determine highly secreting transformants. The transformants exhibiting the highest secreted yields were stored and used as stocks for subsequent expression trials.

2.8. Enzyme activity testing

200 μl of 1 % (w/v) CMC in 0.1 M MTC buffer at the specified pH was combined with 200 μl of appropriately diluted enzyme preparation and incubated for 30 min at 50 °C. 100 μl of each reaction was added to 300 μl of the DNS reagent in a 0.5 mL microcentrifuge tube and the mixture was incubated in a thermal cycler at 99 °C for 5 min and then 4 °C for 5 min. The absorbance of samples at 540 nm (A_{540}) was measured using a BioTek Synergy HT plate reader (BioTek, UK). A_{540} readings for enzyme/sample controls were subtracted from the A_{540} value for each sample. Enzyme/sample controls were set up by incubating 1 % (w/v) CMC without enzyme alongside the other reactions during the 50 °C incubation step. 50 μl of the CMC was then added to 300 μl of the DNS reagent with 50 μl of the relevant enzyme preparation and immediately boiled before a reaction could take place. One unit of enzyme activity was defined as the amount of enzyme required to produce 1 μmol reducing sugar ends, established via a glucose standard curve, per minute at the reaction conditions.

The LPMO assay adapted from Breslmayr et al. (2018) was used to test the activity of TrCel61a. A solution comprised of 860 μl of 116 mM MTC buffer pH 6.0, 100 μl of 100 mM 2,6-dimethoxyphenol (2,6-DMP) and 20 μl of 5 mM H_2O_2 was transferred to a 1.5 mL spectrophotometer cuvette and incubated for 15 min at 30 °C in a Jasco V-530 spectrophotometer. 20 μl of TrCel61a preparation was added to the cuvette and the change in A_{469} was recorded continuously over 480 s, in triplicate. 1 unit of LPMO activity was defined by Breslmayr et al. (2018) as the amount of enzyme converting 2 μmol 2,6-DMP or forming of 1 μmol coerulignone ($\varepsilon 469 = 53{,}200\ M^{-1}\ cm^{-1}$) per min under the given conditions.

2.9. Hydrolysis of cellulosic substrates and cello-oligosaccharide analysis

Enzymatic hydrolysis of cellulosic substrates including RAC, untreated and pretreated *Miscanthus* material was based on the technical report NREL/TP-5100–63351 24 designed for saccharification at small reaction volumes with low solids loading (Resch et al., 2015). Briefly, the equivalent of 14 mg (1 % w/v biomass loading) dry solids were suspended in a volume of 1.4 mL 30 mM sodium acetate buffer (pH 5.5), 0.02 % sodium azide, 1 mg/ml BSA and the tested enzymes, made up to the final volume with deionised water in a 1.6 mL screw-cap microcentrifuge tube for each assay. The tubes were incubated horizontally for up to 72 h in a shaking incubator set to 50 °C (200 rpm) and reactions were stopped by heating samples to 100 °C for 10 min. Samples were analysed for monosaccharide and oligosaccharide yields by High-Performance Anion Exchange Chromatography coupled with Pulsed Amperometric Detection (HPAEC-PAD) with a Dionex ICS-5000 DC chromatography system (Thermo Fisher Scientific, USA). Samples were diluted in ultra-pure (18.2 mΩ) water, filtered through 0.2 μm nylon filters and injected onto the column with a Dionex AS-AP autosampler (Thermo Fisher Scientific, USA). Glucose and DP2-5 COS were separated on a CarboPAC PA1 BioLC™ column (4 × 250 mm, particle size 10 μm) (Thermo Fisher Scientific, USA) via gradient elution over 57 min per sample with the following mobile phases: 0–36 min –100 mM NaOH, 36–42 min – 100 mM NaOH, 1 M NaOAc, 42–57 min – 100 mM NaOH. Eluent flowrate was maintained at 0.3 mL/min. Data were annotated and analysed using Chromeleon® 7. Retention times and concentrations of glucose and DP 2 to 5 COS were determined by running calibration curves from pure standards purchased from Megazyme (Ireland). Due to the variability in the initial glucan content in material from different pretreatment processes (see supplementary material), final sugar concentrations were calculated as g/ g glucan from the dry mass as described by Resch et al. (2015). Hydrolysis factors (H) for measured sugars were 0.9 for glucose, 0.95 for cellobiose, 0.96 for cellotriose, 0.97

for cellotetraose and 0.98 for cellopentaose.

3. Results and discussion

3.1. Enzymatic hydrolysis profiles of COS-producing endoglucanases on amorphous cellulose and determination of enzyme loading

The results of a literature search for endoglucanases either displaying processivity or with minimal activity towards COS, in order not to further degrade them during prolonged hydrolysis have previously been reported (Barbosa et al., 2020). Interestingly, of the five candidates selected, only two enzymes, CtCel9r from *Clostridium thermocellum* and TfCel9a from *Thermobifida fusca*, are classified as GH9 processive endoglucanases and contain the characteristic additional CBM3 motif. A conserved domain search for the remaining three sequences on NCBI (Lu et al., 2020) revealed no further carbohydrate-binding modules, indicating that they were either classic bacterial GH9 endoglucanases or eukaryotic GH45 endoglucanases that were nevertheless shown to produce COS as end-products. Mature coding sequences for the five selected endoglucanases (Table 1) were synthesised, cloned into *P. pastoris* and expressed after isolating transformants secreting the highest titres of functional product for each enzyme. To test the practicality of secreted *Pichia*- based expression of each endoglucanase, whole-cell supernatants were initially tested for endoglucanase activity on CMC using the DNS assay (Fig. 1A). Whilst the enzymes have different reported pH and temperature optima, a standardised condition of 50 °C and pH 5.0 was used for each reaction since this corresponded to the conditions in which they would be used in synergy with other enzymes. The highest CMCase activities observed under these conditions were from CcCel9m, TfCel9a and CaCel, with similar activities ranging between 1.5 and 1.65 U/ml for all three enzymes (Fig. 1A). In comparison, significantly less activity was observed in the TrCel45a and CtCel9r preparations, at 0.82 and 0.55 U/ml respectively. Since the reported optimum pH for TrCel45a is 5.0, and it retains over 90 % of its activity at 50 °C (Karlsson et al., 2002), the low activity could reflect weak expression or secretion from *P. pastoris*, although Karlsson et al (2002) showed that it has an intrinsically low turnover. The temperature optimum of CtCel9r however is ~ 79 °C, which could explain why it exhibited the lowest activity under the tested conditions (Zverlov et al., 2005).

To quantify the yields of individual COS up to DP5 on amorphous cellulose, an endpoint assay was conducted with whole-cell supernatants diluted 1/5 and incubated with 1 % (w/v) RAC for 72 h (Fig. 1B). The CMCase activities recorded for the five enzymes largely correlated with total COS production, with the highest total COS and glucose yields produced from reactions with CcCel9m, TfCel9a and CaCel (~500 to 650 mg/L). In addition, notable differences in the COS profiles were found between the three enzymes (Fig. 1B). Of all the tested enzymes, TfCel9a produced the largest fraction of higher DP COS (DP4 and DP5) at 246 mg/l, comprising 49 % of the total COS measured in the hydrolysate. By comparison, the most abundant COS produced by CaCel was cellobiose (DP2), which comprised ~ 46 % of the total measured COS produced. CcCel9m exhibited the highest specificity, as the total yield of

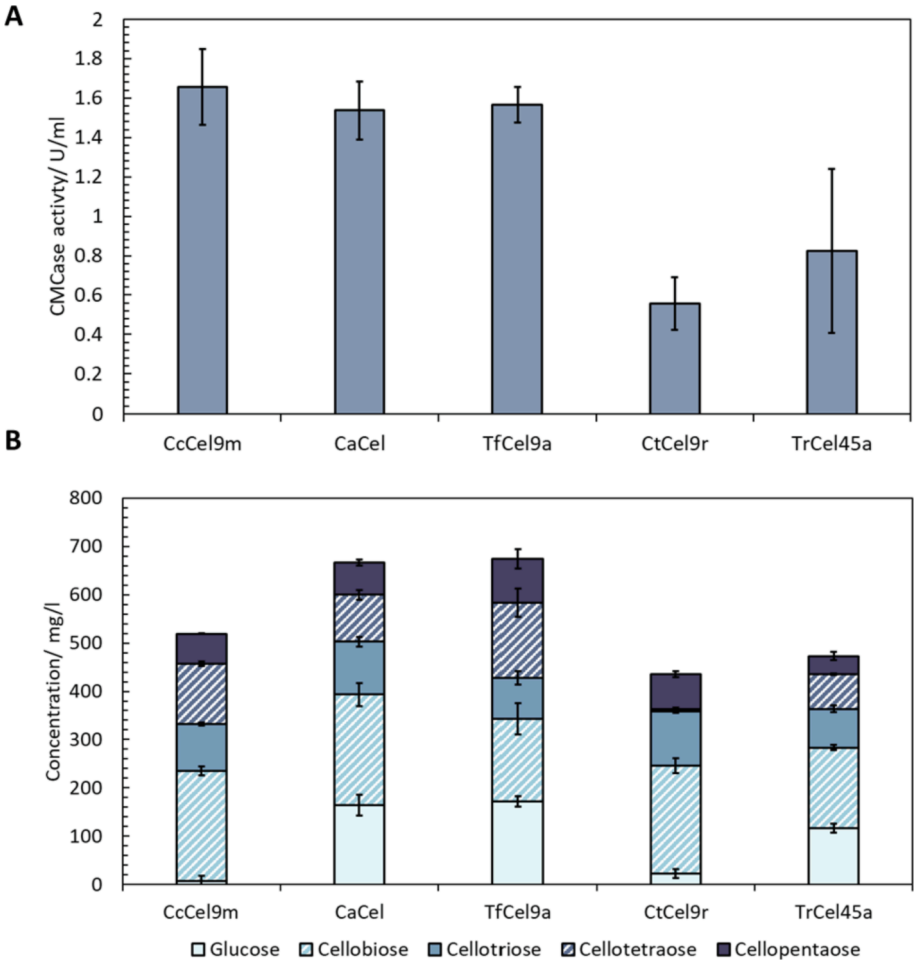

Fig. 1. (A) CMCase activity at 50 °C pH 5.0 of endoglucanases in whole-cell supernatant following expression, and (B) final concentrations of glucose and COS (up to cellopentaose DP5) produced from 1 % RAC following 72 h hydrolysis at 50 °C. pH 5.0 with endoglucanases in whole cell supernatants diluted 1:5. Error bars represent standard deviation (n = 3).

COS produced was comparable to that of TfCel9a and CaCel, but with a significantly lower glucose fraction (Fig. 1B). The varying COS profiles of the selected endoglucanases on amorphous cellulose highlights their potential as a toolset to control the DP of COS-rich hydrolysates to suit the end application. CaCel and TfCel9a can be selected to generate larger fractions of DP2-3 or DP4-5 COS respectively, whereas CcCel9m could be considered in applications where minimal conversion of cellulose to glucose is required.

Despite confirming the hydrolysis of RAC to COS (Fig. 1B), total hydrolysis of the available glucan was low, with the highest percentage conversion of RAC to glucose and DP2 to 5 COS of ~ 7 % being achieved by TfCel9a and CaCel. This was at least partly due to the low enzyme loading from the low initial concentration in crude, whole-cell supernatant. In the case of TfCel9a, this was approximately 0.3 U/ml, corresponding to 30 U per g glucan in the previous reaction. To confirm this, TfCel9a was concentrated and buffer exchanged to a final concentration of 14 ± 1 U/ml. The pH optimum of TfCel9a was also found to be 5.5 after conducting a series of DNS assays between pH 5.0 and 7.0. Hydrolysis of 1 % RAC was repeated with an increased loading of 3 U/ml TfCel9a at pH 5.5 and COS yields were compared to hydrolysis by the original loading of 0.3 U/ml (Fig. 2A). Increasing enzyme loading resulted in a less than stoichiometric > 3-fold increase in the hydrolysis of 1 % RAC, with the highest final COS concentration observed after 72 h at ~ 2 g/l. However, a shift in the product profile towards larger fractions of lower DP COS, and a decrease in DP4 and 5 COS was also observed, with no quantifiable cellopentaose (DP5) detected after 72 h. This is consistent with the well-studied mechanism of hydrolysis by TfCel9a, which has been demonstrated to initially cleave cellotetraose (DP4) from cellulose chains in a processive manner, but eventually hydrolyse this further to produce cellotriose, cellobiose and glucose (Kostylev and Wilson, 2014). Increasing the concentration of TfCel9a probably drove the latter reaction due to increased concentrations of higher DP COS initially being produced in the reaction; sequential hydrolysis would be consistent with the less than stoichiometric increase in glucan degradation. To determine whether higher titres of DP4 to 5 COS could be obtained by increasing the availability of amorphous cellulose binding sites, the initial concentration of RAC was increased from 1 % to 2 % (Fig. 2B). At the 24 h time point, a larger cellotetraose fraction was observed compared to that obtained with 1 % RAC, indicating a lower rate of further hydrolysis in comparison to its initial production. However, after prolonged hydrolysis, cellotetraose titres decreased from ~ 428 mg/l at 24 h to ~ 302 mg/l at 72 h while cellobiose production increased by over 60 % in the same time to reach 1556 mg/l. Titres of cellopentaose also remained negligible. Whilst the final concentration of COS was higher, the total yield from hydrolysis of 2 % was also diminished in comparison to 1 % RAC. Quantified hydrolysis products accounted for < 16 % of the total glucan available in the reaction with 2 % RAC in comparison to 24 % for 1 % RAC, suggesting that the enzyme

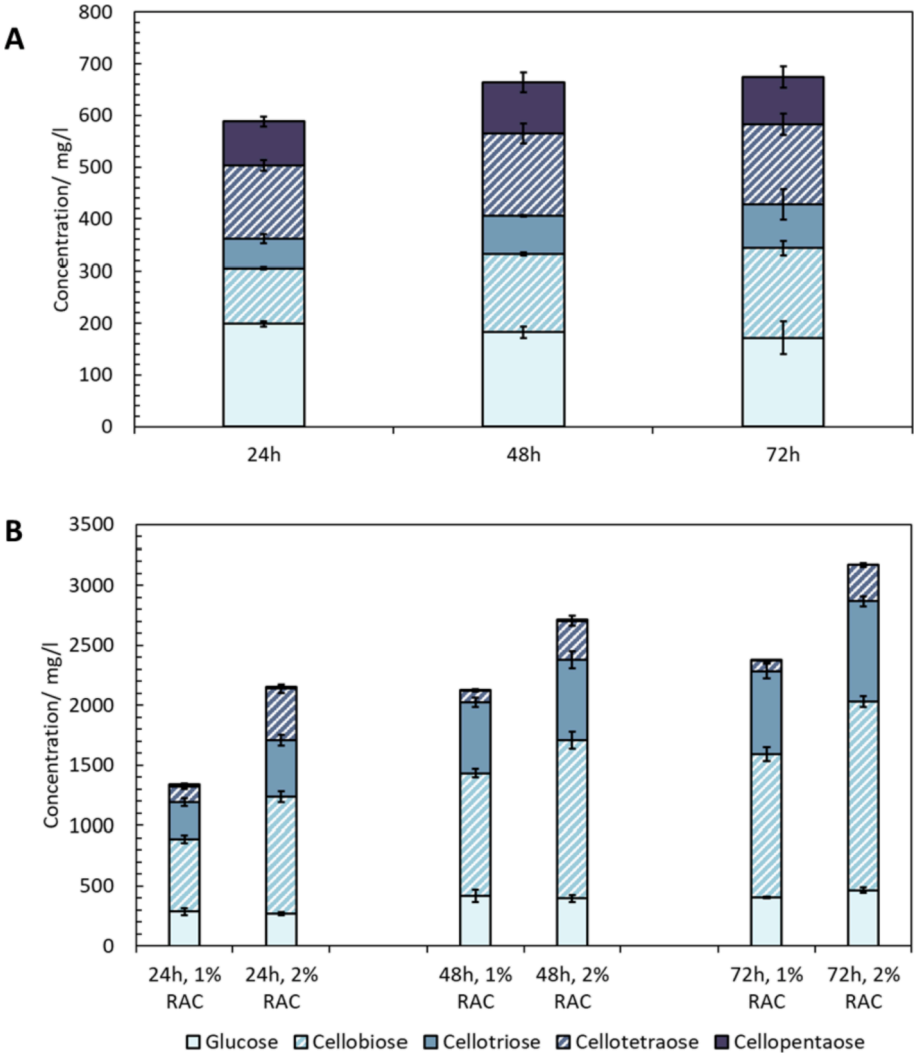

Fig. 2. Glucose and COS production (up to DP5) after 24, 48 and 72 h following hydrolysis at 50 °C, pH 5.5 (A) of 1 % RAC with 0.3U/ml TfCel9a from whole culture supernatant, and (B) of 1 % and 2 % RAC with 3 U/ml TfCel9a following partial purification and buffer exchange. Error bars represent standard deviation (n = 3).

loading had become limiting. These results show that while TfCel9a can selectively produce COS up to DP4, the higher DP COS can only be recovered at low substrate conversions or in a membrane reactor, where the product is continually removed, prohibiting further reaction with the enzyme.

3.2. Synergistic enzymatic hydrolysis of H_3PO_4 pretreated Miscanthus by endoglucanases TfCel9a and CcCel9m with a modified cellobio/triohydrolase and LPMO

Having individually confirmed the five endoglucanases activities on a lignin-free model cellulose substrate, confirmation of enzymatic saccharification by the recombinant endoglucanases on a lignocellulosic material was required. *Miscanthus* is an established and agronomically viable lignocellulosic biomass resource for bioconversion into bio-fuels, bio-based materials and chemicals, including co-firing in power stations within Europe as well as the production of renewable cellulosic ethanol and bioplastics amongst many others (Bhatia et al., 2019; Lee and Kuan, 2015). As such, the high biomass yielding (~14 t/ha) and seed-based (high multiplication rates and lower establishment costs) hybrid *Miscanthus Mx2779* was selected as a lignocellulosic substrate to test for synergistic COS release from endoglucanases in combination with assistive enzymes. To produce increased yields of higher DP COS with a minimal glucose fraction, the endoglucanases TfCel9a and CcCel9m were selected. Synergism between processive and classic endoglucanases has previously been reported, and increased COS yields with enzyme cocktails containing both TfCel9a and CcCel9m on a crystalline lignocellulosic substrate have been demonstrated (Barbosa et al., 2020; Watson et al., 2009). Furthermore, enzyme activity tests on CMC confirmed that TfCel9a and CcCel9m had a shared pH optimum of 5.5. After a 20-minute H_3PO_4 pretreatment step to generate swollen cellulose (Zhang et al., 2006), COS release from *Miscanthus Mx2779* was measured following a 72-hour incubation with TfCel9a and CcCel9m, individually and in combination, using the previously tested enzyme loadings of 300 and 150 CMCase U/g solids in order not to limit saccharification. Hydrolysis was also performed on untreated *Miscanthus* biomass as a control to assess the impact of the H_3PO_4 pretreatment on COS yields (Fig. 3). As expected, yields on untreated *Miscanthus* were low for each condition, with a maximum of < 50 mg/g glucan total sugars (DP1 to 5) released (Fig. 3A). The largest fraction of released sugars for each enzyme combination was glucose, suggesting that the rate of secondary hydrolysis of released COS was exceeding the rate of

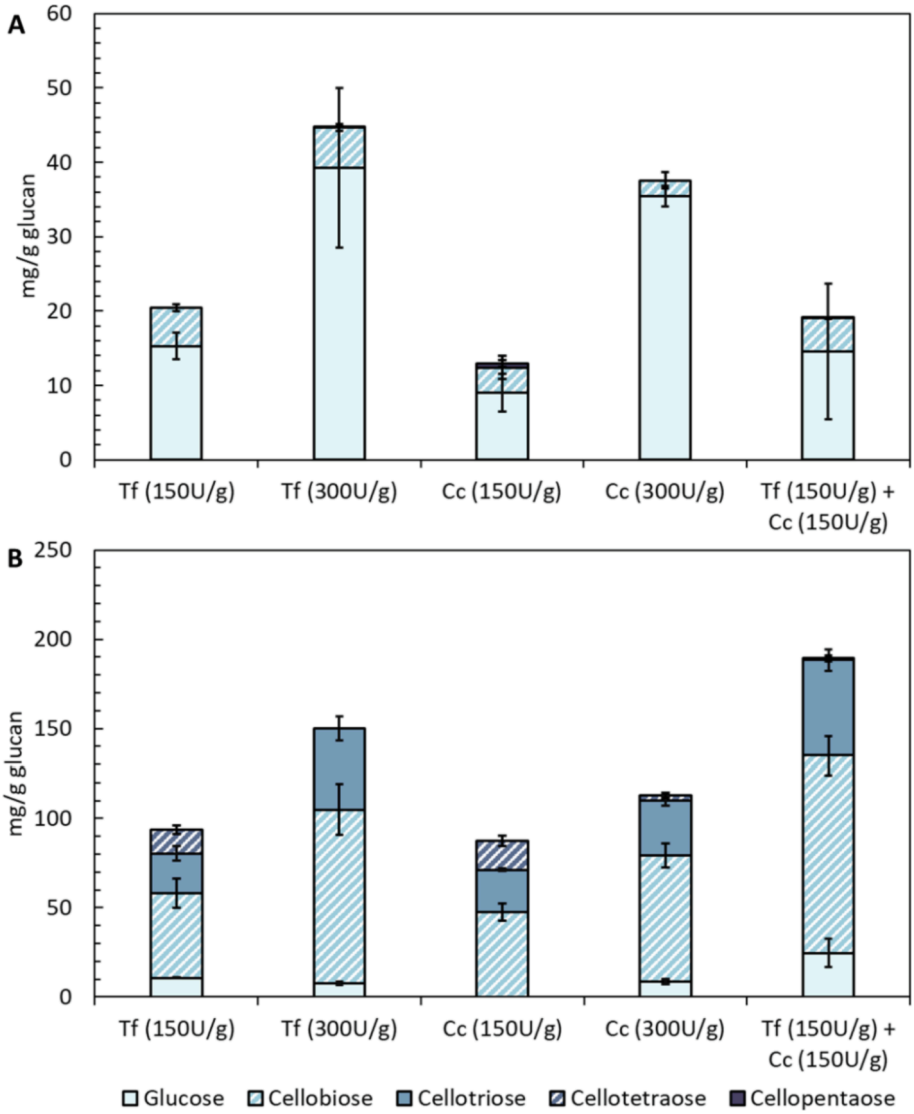

Fig. 3. Glucose and COS production (up to DP5) from combinations of TfCel9a and CcCel9m at enzyme loadings of 150 or 300 CMCase Units/g solids incubated at 50 °C, pH 5.5 using 1 % (w/v) (A) untreated *Miscanthus*, and (B) phosphoric acid pretreated (20 min) *Miscanthus*. Tf: TfCel9a, Cc: CcCel9m. Error bars represent standard deviation (n = 3).

soluble COS release from cellulose. Total saccharification was significantly increased following H_3PO_4 pretreatment of *Miscanthus* (Fig. 3), although total sugars released from the single enzyme reaction of 300 U/g TfCel9a was lower than on RAC (150 compared to ~ 240 mg/g glucan). However, the COS profiles were comparable. Doubling the enzyme loading from 150 U/g to 300 U/g solids resulted in ~ 50 % increase in total COS yield for TfCel9a and ~ 30 % for CcCel9m, with a reduction in cellotetraose and concurrent increases in cellotriose and cellobiose fractions for both enzymes (Fig. 3B). Incubation of H_3PO_4 pretreated *Miscanthus* with a combined loading of 150 U/g TfCel9a and 150 U/g CcCel9m resulted in higher COS release compared to the equivalent loading of the individual enzymes, confirming that the two endoglucanases, TfCel9a and CcCel9m, function synergistically. Whilst the combination of TfCel9a and CcCel9m produced more glucose in comparison to 300 U/g TfCel9a or CcCel9m alone, it remained a minor fraction of the total COS products. Interestingly, the addition of 150 U/g CcCel9m and 150 U/g TfCel9a to untreated *Miscanthus* resulted in similar yields to that achieved with 150 U/g TfCel9a alone (Fig. 3A). This observation indicates that these two enzymes only exhibit synergy on amorphous regions of cellulose generated through the H_3PO_4 pretreatment, while also confirming that TfCel9a has some activity of native cellulose due to the presence of the additional carbohydrate binding module (Kostylev and Wilson, 2014). Part of the synergy between TfCel9a and CcCel9m must derive from the ability of CcCel9m to cleave the amorphous cellulose internally, generating more ends for the TfCel9a to work on, but the reported ability of CcCel9m to produce COS could also reflect a lower tendency to further hydrolyse the soluble COS to shorter DP products.

The classical mechanism for efficient enzymatic hydrolysis of crystalline cellulose requires an *exo*-acting glucanase, which typically releases the repeating unit, cellobiose from the ends of cellulose chains. However, a truncated mutant of a cellobiohydrolase (exoglucanase) from *Orpinomyces* sp.Y102, OsCelC7(−105) has been shown to have a rare cellobio/triohydrolase activity, releasing cellobiose and cellotriose from amorphous cellulose. This mutant lacks the N-terminal 105 amino acid residues that comprise the non-catalytic, putative dockerin domains and was found to be better expressed as a soluble protein from heterologous hosts than the full-length protein (Chen et al., 2014). To test its possible application as an assistive exoglucanase for COS production with TfCel9a and/or CcCel9m, OsCelC7(−105) was also cloned and expressed in *P. pastoris* to a final CMCase activity of 10.6 ± 0.6 U/ml at pH 5.5, 50 °C, following concentration and buffer exchange via ultrafiltration. Additionally, the AA9 LPMO TrCel61a from *Trichoderma reesei* was expressed in *P. pastoris*, concentrated by ultrafiltration and confirmed to exhibit activity via the 2,6-DMP assay under the test condition of 50 °C, pH 5.5. To analyse their impact on hydrolysis, TrCel61a and OsCelC7 preparations were added at concentrations of 5 mg/g solids and 150 CMCase U/g solids respectively, with 1 mM ascorbic acid added as an electron donor for TrCel61a, to untreated and H_3PO_4 pretreated *Miscanthus* together with TfCel9a and CcCel9m (Fig. 4).

OsCelC7(−105) significantly increased COS release from both untreated and H_3PO_4 pretreated *Miscanthus* when added together with TfCel9a and CcCel9m, with the increased yield on H_3PO_4 pretreated *Miscanthus* comprised mainly of cellobiose. Cellotriose yields did not

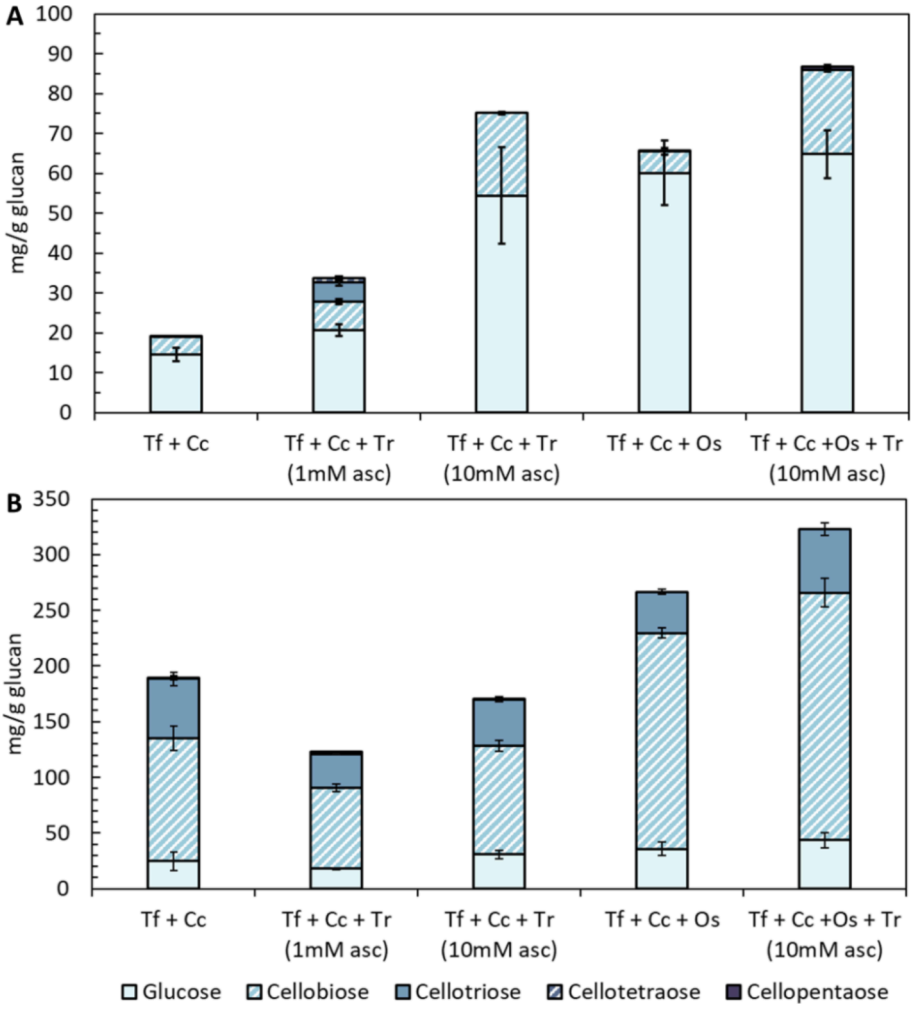

Fig. 4. Glucose and COS production (up to DP5) from combinations of TfCel9a, CcCel9m, TrCel61a and OsCelC7(−105) incubated at 50 °C, pH 5.5 at enzyme loadings of 150 CMCase Units/g solids for TfCel9a, CcCel9m and OsCelC7(−105) and 5 mg/g solids for TrCel61a, using 1 % (w/v) (A) untreated *Miscanthus*, and (B) phosphoric acid pretreated (20 min) *Miscanthus*. Tf: TfCel9a, Cc: CcCel9m, Os: OsCelC7 (−105), Tr: TrCel61a, asc: ascorbic acid. Error bars represent standard deviation (n = 3).

increase proportionally and the final yield of cellotriose decreased to 37.0 ± 2.1 mg/g glucan from 53.4 ± 6.0 mg/g glucan (Fig. 4B), supporting previous findings that OsCelC7(−105) could hydrolyse cellotriose to cellobiose and glucose over extended periods (Chen et al., 2014). However, glucose formation still remained low, increasing by ~ 11 mg/g glucan and accounting for ~ 13 % of the measured hydrolysate.

TrCel61a markedly improved saccharification of untreated *Miscanthus* for all conditions in which it was introduced, resulting in ~ 50 % increase when added with TfCel9a and CcCel9m, although total COS yields remained low and glucose was still the major product (Fig. 4A). This trend was not observed for H_3PO_4 pretreated *Miscanthus*, with a reduction in overall yield found when TrCel61a was added with TfCel9a and CcCel9m (Fig. 4B). To test whether the concentration of the electron donor was limiting activity on H_3PO_4 pretreated *Miscanthus*, the concentration of ascorbic acid was increased to 10 mM in combinations of TrCel61a with TfCel9a + CcCel9m, TfCel9a alone and CcCel9m + OsCelC7(−105). COS yield improved for TfCel9a + CcCel9m + TrCel61a on untreated *Miscanthus* with increased ascorbic acid but did not outperform TfCel9a + CcCel9m alone on H_3PO_4 pretreated material. However, the addition of both OsCelC7(−105) and TrCel61a with 10 mM ascorbic acid resulted in the highest level of saccharification observed for both untreated and H_3PO_4 pretreated *Miscanthus*, increasing the total DP1 to 5 sugar yield from H_3PO_4 pretreated *Miscanthus* by ~ 70 % to 323 mg/g glucan. COS production was even improved compared to the three-enzyme combination of TfCel9a + CcCel9m + OsCelC7(−105) despite the observation that TrCel61a reduced COS production using TfCel9a + CcCel9m when added alone. Final cellotriose yields (57.1 ± 6.0 mg/g glucan) were also higher in comparison to TfCel9a + CcCel9m + OsCelC7(−105), suggesting that the four candidate enzymes work synergistically to release COS from glucan that was previously inaccessible to endoglucanases alone. Importantly, all of the enzymes were functional under a single set of reaction conditions and are therefore compatible as a tailor-made enzyme cocktail for enzyme-mediated production of COS.

3.3. Pretreatment by steam explosion or [C_2mim] [OAc] increases COS yields by TfCel9a, CcCel9m, OsCelC7(−105) and TrCel61a enzyme cocktails

Additional pre-treatment processes were investigated on *Miscanthus Mx2779*, particularly aiming to increase the amorphous cellulose content and accessibility to the cellulolytic enzyme cocktail (TfCel9a, CcCel9m, OsCelC7(−105) and TrCel61a) for optimised COS production. Firstly, the H_3PO_4 pretreatment exposure was increased from 20 to 45 min to enhance disruption of the lignin-carbohydrate complex bonds and the crystalline structure of cellulose as well as to remove lignin and the partially hydrolysed hemicellulose fragments (see Supplementary Materials) under modest pretreatment conditions (50 °C) (Zhu et al., 2009). Both H_3PO_4 reaction conditions were also trialled with and without a combinatorial steam explosion (SE) pretreatment step, as SE is an effective and universally applicable pretreatment method that can solubilise the hemicellulose fraction into high-value xylo-oligosaccharides as well as facilitate the exposure of cellulose to enzymes and solvents (Bhatia et al., 2020; Bhatia et al., 2021). Finally the H_3PO_4 was

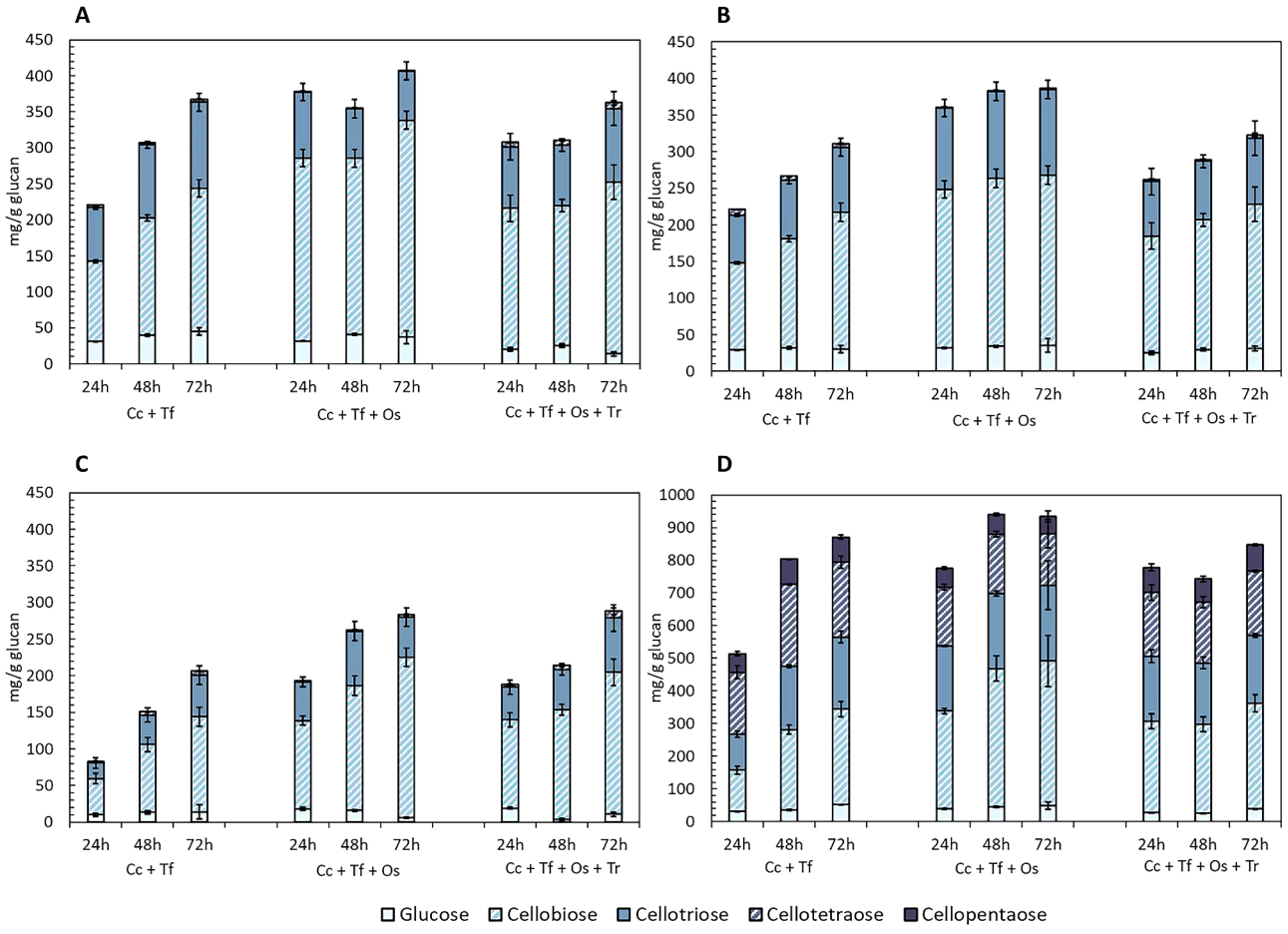

Fig. 5. Glucose and COS production (up to DP5) from *Miscanthus* after different pretreatments, using enzyme combinations of TfCel9a (150 U/g solids), CcCel9m (150 U/g solids), OsCelC7(−105) (150 U/g solids) and TrCel61a (5 mg/g solids, 10 mM ascorbic acid) at 50 °C, pH 5.5 for24, 48 and 72 h. (A) H_3PO_4 pretreated (45 min), (B) steam explosion and H_3PO_4 (20 min), (C) steam explosion and H_3PO_4 (45 min), (D) [C2mim][OAc] pretreated. Tf: TfCel9a, Cc: CcCel9m, Os: OsCelC7 (−105), Tr: TrCel61a. Error bars represent standard deviation (n = 3).

replaced with the IL [C_2mim][OAc], selected based on its additional lignin dissolving properties as well as having been previously established as a suitable pretreatment to support endoglucanase hydrolysis of *Miscanthus Mx2779* (Bhatia et al., 2021). The four new starting materials were hydrolysed with the best performing enzyme combinations identified previously, TfCel9a + CcCel9m, TfCel9a + CcCel9m + OsCelC7 (−105) and TfCel9a + CcCel9m + OsCelC7(−105) + TrCel61a (Fig. 5).

Incorporating SE into the original 20 min H_3PO_4 pretreatment step or increasing H_3PO_4 reaction time to 45 min improved COS yields from the TfCel9a + CcCel9m and TfCel9a + CcCel9m + OsCelC7(−105) cocktails, although yields from TfCel9a + CcCel9m + OsCelC7(−105) + TrCel61a remained largely unchanged (Fig. 5B and A, respectively). For both materials, the highest total saccharification was achieved with TfCel9a + CcCel9m + OsCelC7(−105), increasing from ~ 267 mg/g glucan (20 min H_3PO_4) to 387 and 407 mg/g glucan (on the SE + 20 min and 45 min H_3PO_4 respectively). Whilst COS release increased linearly for reactions with just TfCel9a + CcCel9m, between 24 and 72 h, only minor increases in yield were observed for TfCel9a + CcCel9m + OsCelC7 (−105) after 24 h, suggesting that shorter reaction times could be used with this combination, while still achieving optimal hydrolysis. The COS profile from TfCel9a + CcCel9m + OsCelC7(−105) on 45 min H_3PO_4 treated material remained similar to the 20 min H_3PO_4 material after 72 h, with cellotriose and cellobiose making up the largest fractions, comprising ~ 17 % and 74 % of the total hydrolysate, respectively. Interestingly, the same hydrolysis on the combinatorial SE and 20 min H_3PO_4 treated material yielded a much larger cellotriose fraction of ~ 30 % that remained stable throughout the 72 h period. The results indicate that SE pretreatment facilitated enzyme access to the cellulose, possibly through higher lignin removal and changes in the cellulose structure (see Supplementary Material), thereby reducing the undesired further hydrolysis of the released cellotriose to cellobiose and glucose. However, the combination of both SE and 45 min H_3PO_4 pretreatment resulted in lower yields, with none of the enzyme cocktails trialled producing over 300 mg/g glucan of DP1 to5 glucose sugars. Whilst unexpected, since a higher extraction of xylan and lignin was achieved by the combinatorial SE and 45 min H_3PO_4 pretreatment method and a shift in the relative amorphous and crystalline cellulose abundance was achieved (see Supplementary Material), the results indicate an interaction between both process steps that should be considered when designing future pretreatment strategies for enzyme-mediated production of COS.

Whilst it appeared that the addition of TrCel61a had little effect on saccharification of *Miscanthus* following the more severe pretreatment steps, HPAEC analysis of reactions containing TrCel61a revealed the presence of additional peaks most likely corresponding to oxidised oligosaccharides that were not factored into the final product (see Supplementary material). It is not known whether the presence of oxidised oligosaccharides mixed with COS would be benign, detrimental or useful for the purposes envisaged. However, with a focus purely on COS production the results indicate that, with further physicochemical processing of lignocellulose, specifically to increase amorphous cellulose content and cellulose exposure, LPMO activity becomes less useful, and potentially detrimental as portions of the hydrolysable glucan is converted to oxidised sugars.

Enzymatic hydrolysis of the available glucan was dramatically increased following pretreatment with [C_2mim][OAc], with a maximum conversion of 933 mg/g into DP1 to 5 glucose sugars by the TfCel9a + CcCel9m + OsCelC7(−105) cocktail (Fig. 5D). In a similar pattern to its reaction with the other pre-treated materials, maximum hydrolysis was achieved by TfCel9a + CcCel9m + OsCelC7(−105) after 48 h, although the COS profile remained stable for up to 72 h, showing minimal conversion of higher DP COS to cellobiose and glucose. In addition to higher yields, the COS profiles were also more varied for all enzyme cocktails, with the higher DP oligosaccharides cellotetraose and cellopentaose comprising significant fractions of the total hydrolysate and, although unquantified, additional peaks were observed on the corresponding HPAEC chromatogram, indicating the presence of small quantities of larger COS such as cellohexaose. Since cellulose crystallinity has been identified as a strong indicator of cellulase performance (Hall et al., 2010), and the activity of each of the enzymes used in this study on crystalline cellulose (untreated biomass) has been demonstrated to be weak (Fig. 4A), [C_2mim][OAc] was inferred to provide the highest conversion of crystalline into amorphous or less recalcitrant forms of cellulose (Cheng et al., 2012). In fact, greatly improved enzymatic saccharification performance following pretreatment involving ILs such as [C_2mim][OAc] has been reported using a number of cellulosic substrates including Avicel, sugarcane bagasse and *Miscanthus*, with typical conversions of available glucan to reducing sugars ranging between 80 and 100 % (Cheng et al., 2011; Karatzos et al., 2012; Li et al., 2013). Saccharification of [C_2mim][OAc] pre-treated *Miscanthus Mx2779* with the commercial enzyme preparation Cellic CTec2 similarly gave a 93 % conversion of the total glucan to glucose (Bhatia et al., 2021). The results demonstrate that pretreatment using [C_2mim][OAc] can facilitate efficient COS production via selected recombinant enzymes and allows greater control over product specificity with minimal glucose release as a by-product, while maintaining the same efficiency of saccharification as commercial enzyme benchmarks. Whether this represents the most economic route for the production of COS requires more detailed technoeconomic analysis. Compositional analysis (see Supplementary Material) shows that a lower percentage of the initial glucan is recovered after [C_2mim][OAc] treatment compared to H_3PO_4 treatment, with or without initial SE. Based on initial glucan content the yield of COS after [C_2mim][OAc] pretreatment is ~ 80%, whereas the best yields based on H_3PO_4 and SE pretreatment were approaching 40% (and could probably be improved). Given the cost of [C_2mim][OAc] treatment, the latter may prove to be preferable from an economic perspective, particularly as phosphate salts generated at the end of the pretreatment process could be recycled for use as fertilisers, nutrients for microorganisms or fermentation process buffers. However, as demonstrated, the COS profile can be affected by the pretreatment route selected.

The ability to obtain high yields of high DP COS after [C_2mim][OAc] pretreatment suggests a synergistic benefit of TfCel9a, CcCel9m and OsCelC7(−105) as a cellulolytic cocktail which goes beyond simple hydrolytic rate enhancement, as it is clear that with amorphous cellulose, the competition between COS and cellulose hydrolysis has shifted to favour the latter, despite the increasing concentration of COS appearing through the reaction. While the synergy between CcCel9m and TfCel9a partially reflects the ability of CcCel9m to generate new ends for TfCel9a to work on, the fact that CcCel9m alone is known to generate COS suggests that its affinity for the released COS is lower than many other endoglucanases. The presence of the truncated cellobiohydrolase OsCelC7 (−105) clearly accelerated this process, although the yields of cello-oligomers with and without OsCelC7(−105) after 48 and 72 h, respectively, were similar (Fig. 5D). This could simply reflect the increased rate of cello-oligomer generation resulting from a combination of TfCel9a and OsCelC7(−105) working on both the non-reducing and reducing ends (respectively) generated by CcCel9m, and the higher proportion of cellobiose generated by the three, compared to the two enzyme combination supports this. However, it could also reflect a different synergy, where OsCelC7(−105) selectively binds to the DP4 to 5 products coming from the initial action of TfCel9a, thus outcompeting the TfCel9a and freeing it to generate more DP4 to 5 rather than hydrolysing the COS.

4. Conclusions

COS substrates have potential to be utilised in a number of modern applications including bioethanol production and as prebiotic supplements. This study demonstrated synergisms between combinations of cellulases TfCel9a, CcCel9m, OsCel7a(−105) and TrCel61a for enzyme-mediated COS production from *Miscanthus* and demonstrated how their effectiveness depends on the nature and extent of pretreatment. The IL

[C_2mim][OAc] was the most favourable pretreatment tested to reduce biomass recalcitrance and enhance cellulose accessibility for high yield COS production, achieving ~ 90 % conversion of the glucan to COS (DP 2 to 5). These results are informative for creating new COS production opportunities for industrial applications.

CRediT authorship contribution statement

Emanuele G. Kendrick: Validation, Investigation, Writing – original draft, Writing – review & editing, Visualization, Project administration. **Rakesh Bhatia:** Validation, Investigation, Writing – original draft, Writing – review & editing, Visualization. **Fernando C. Barbosa:** Validation, Investigation, Visualization. **Rosanna Goldbeck:** Validation, Writing – review & editing, Supervision. **Joe A. Gallagher:** Validation, Writing – review & editing, Supervision, Funding acquisition. **David J. Leak:** Conceptualization, Validation, Writing – original draft, Writing – review & editing, Supervision, Funding acquisition.

Declaration of competing interest

The authors declare that they have no known competing financial interests or personal relationships that could have influenced the work reported in this paper.

Acknowledgements

Funding: This work was supported by the Biotechnology and Biological Sciences Research BBSRC (UK) [grant number BB/P017460/1] and São Paulo Research Foundation, FAPESP (Brazil) [grant number 2015/50612-8]. In addition, the authors thank the BEACON Biorefining Centre for supportive work.

Appendix A. Supplementary data

Supplementary data to this article can be found online at https://doi.org/10.1016/j.biortech.2022.127399.

References

Almagro Armenteros, J.J., Tsirigos, K.D., Sønderby, C.K., Petersen, T.N., Winther, O., Brunak, S., von Heijne, G., Nielsen, H., 2019. SignalP 5.0 improves signal peptide predictions using deep neural networks. Nat. Biotechnol. 37 (4), 420–423.

Ávila, P.F., Silva, M.F., Martins, M., Goldbeck, R., 2021. Cello-oligosaccharides production from lignocellulosic biomass and their emerging prebiotic applications. World J. Microbiol. Biotechnol. 37, 73.

Aw, R., Polizzi, K.M., 2016. Liquid PTVA: a faster and cheaper alternative for generating multi-copy clones in *Pichia pastoris*. Microb. Cell Fact. 15, 29.

Barbosa, F.C., Kendrick, E., Brenelli, L.B., Arruda, H.S., Pastore, G.M., Rabelo, S.C., Damasio, A., Franco, T.T., Leak, D., Goldbeck, R., 2020. Optimization of cello-oligosaccharides production by enzymatic hydrolysis of hydrothermally pretreated sugarcane straw using cellulolytic and oxidative enzymes. Biomass Bioenergy 141, 105697.

Basílio, A.C.M., de Araújo, P.R.L., de Morais, J.O.F., da Silva Filho, E.A., de Morais, M.A., Simões, D.A., 2008. Detection and identification of wild yeast contaminants of the industrial fuel ethanol fermentation process. Curr. Microbiol. 56 (4), 322–326.

Béguin, P., Aubert, J.P., 1994. The biological degradation of cellulose. FEMS Microbiol. Rev. 13, 25–58.

Belaich, A., Parsiegla, G., Gal, L., Villard, C., Haser, R., Belaich, J.-P., 2002. Cel9M, a new family 9 cellulase of the *Clostridium cellulolyticum* cellulosome. J. Bacteriol. 184 (5), 1378–1384.

Bhatia, S.K., Gurav, R., Choi, T.-R., Jung, H.-R., Yang, S.-Y., Moon, Y.-M., Song, H.-S., Jeon, J.-M., Choi, K.-Y., Yang, Y.-H., 2019. Bioconversion of plant biomass hydrolysate into bioplastic (polyhydroxyalkanoates) using *Ralstonia eutropha* 5119. Bioresour. Technol. 271, 306–315.

Bhatia, R., Winters, A., Bryant, D.N., Bosch, M., Clifton-Brown, J., Leak, D., Gallagher, J., 2020. Pilot-scale production of xylo-oligosaccharides and fermentable sugars from *Miscanthus* using steam explosion pre-treatment. Bioresour. Technol. 296, 122285.

Bhatia, R., Lad, J.B., Bosch, M., Bryant, D.N., Leak, D., Hallett, J.P., Franco, T.T., Gallagher, J.A., 2021. Production of oligosaccharides and biofuels from *Miscanthus* using combinatorial steam explosion and ionic liquid pre-treatment. Bioresour. Technol. 323, 124625.

Borges, D.G., Baraldo Junior, A., Farinas, C.S., de Lima Camargo Giordano, R., Tardioli, P.W., 2014. Enhanced saccharification of sugarcane bagasse using soluble cellulase supplemented with immobilized β-glucosidase. Bioresour. Technol. 167, 206–213.

Breslmayr, E., Hanžek, M., Hanrahan, A., Leitner, C., Kittl, R., Šantek, B., Oostenbrink, C., Ludwig, R., 2018. A fast and sensitive activity assay for lytic polysaccharide monooxygenase. Biotechnol. Biofuels 11, 1–13.

Chen, Y.C., Chen, W.T., Liu, J.C., Tsai, L.C., Cheng, H.L., 2014. A highly active beta-glucanase from a new strain of rumen fungus *Orpinomyces sp.*Y102 exhibits cellobiohydrolase and cellotriohydrolase activities. Bioresour. Technol. 170, 513–521.

Cheng, G., Varanasi, P., Li, C., Liu, H., Melnichenko, Y.B., Simmons, B.A., Kent, M.S., Singh, S., 2011. Transition of cellulose crystalline structure and surface morphology of biomass as a function of ionic liquid pretreatment and its relation to enzymatic hydrolysis. Biomacromolecules 12 (4), 933–941.

Cheng, G., Varanasi, P., Arora, R., Stavila, V., Simmons, B.A., Kent, M.S., Singh, S., 2012. Impact of ionic liquid pretreatment conditions on cellulose crystalline structure using 1-ethyl-3-methylimidazolium acetate. J. Phys. Chem. B 116 (33), 10049–10054.

Chu, Q., Li, X., Xu, Y., Wang, Z., Huang, J., Yu, S., Yong, Q., 2014. Functional cello-oligosaccharides production from the corncob residues of xylo-oligosaccharides manufacture. Proc. Biochem. 49 (8), 1217–1222.

de Amorim Araújo, J., Ferreira, T.C., Rubini, M.R., Duran, A.G.G., De Marco, J.L., de Moraes, L.M.P., Torres, F.A.G., 2015. Coexpression of cellulases in *Pichia pastoris* as a self-processing protein fusion. AMB Express 5, 1–10.

Galazka, J.M., Tian, C., Beeson, W.T., Martinez, B., Glass, N.L., Cate, J.H.D., 2010. Cellodextrin transport in yeast for improved biofuel production. Science 330 (6000), 84–86.

Gibson, D.G., Young, L., Chuang, R.-Y., Venter, J.C., Hutchison, C.A., Smith, H.O., 2009. Enzymatic assembly of DNA molecules up to several hundred kilobases. Nat. Meth. 6 (5), 343–345.

Hall, M., Bansal, P., Lee, J.H., Realff, M.J., Bommarius, A.S., 2010. Cellulose crystallinity–a key predictor of the enzymatic hydrolysis rate. FEBS J. 277, 1571–1582.

Hames, B, Ruiz, R, Scarlata, C, Sluiter, A, Sluiter, J, Templeton, D, 2008. Preparation of samples for compositional analysis. Laboratory analytical procedure (LAP). Technical Report NREL/TP-510-42620.

Henrissat, B., Driguez, H., Viet, C., Schülein, M., 1985. Synergism of cellulases from *Trichoderma reesei* in the degradation of cellulose. Bio/Technology 3 (8), 722–726.

Hsieh, C.-W., Cannella, D., Jørgensen, H., Felby, C., Thygesen, L.G., 2014. Cellulase inhibition by high concentrations of monosaccharides. J. Agric. Food Chem. 62 (17), 3800–3805.

Hu, M.L., Zha, J., He, L.W., Lv, Y.J., Shen, M.H., Zhong, C., Li, B.Z., Yuan, Y.J., 2016. Enhanced bioconversion of cellobiose by industrial *Saccharomyces cerevisiae* used for cellulose utilization. Front. Microbiol. 7, 1–11.

Irwin, D., Shin, D.-H., Zhang, S., Barr, B.K., Sakon, J., Karplus, P.A., Wilson, D.B., 1998. Roles of the catalytic domain and two cellulose binding domains of *Thermomonospora fusca* E4 in cellulose hydrolysis. J. Bacteriol. 180 (7), 1709–1714.

Jiao, L.F., Song, Z.H., Ke, Y.L., Xiao, K., Hu, C.H., Shi, B., 2014. Cello-oligosaccharide influences intestinal microflora, mucosal architecture and nutrient transport in weaned pigs. Anim. Feed Sci. Technol 195, 85–91.

Karatzos, S.K., Edye, L.A., Doherty, W.O.S., 2012. Sugarcane bagasse pretreatment using three imidazolium-based ionic liquids; mass balances and enzyme kinetics. Biotechnol. Biofuels 5, 1–12.

Karlsson, J., Siika-aho, M., Tenkanen, M., Tjerneld, F., 2002. Enzymatic properties of the low molecular mass endoglucanases Cel12A (EG III) and Cel45A (EG V) of *Trichoderma reesei*. J. Biotechnol. 99 (1), 63–78.

Karnaouri, A., Muraleedharan, M.N., Dimarogona, M., Topakas, E., Rova, U., Sandgren, M., Christakopoulos, P., 2017. Recombinant expression of thermostable processive MtEG5 endoglucanase and its synergism with MtLPMO from *Myceliophthora thermophila* during the hydrolysis of lignocellulosic substrates. Biotechnol. Biofuels 10, 1–17.

Karnaouri, A., Matsakas, L., Bühler, S., Muraleedharan, M.N., Christakopoulos, P., Rova, U., 2019. Tailoring celluclast® cocktail's performance towards the production of prebiotic cello-oligosaccharides from waste forest biomass. Catalysts 9, 897.

Kim, H., Oh, E.J., Lane, S.T., Lee, W.H., Cate, J.H.D., Jin, Y.S., 2018. Enhanced cellobiose fermentation by engineered *Saccharomyces cerevisiae* expressing a mutant cellodextrin facilitator and cellobiose phosphorylase. J. Biotechnol. 275, 53–59.

Kostylev, M., Wilson, D., 2014. A distinct model of synergism between a processive endocellulase (TfCel9A) and an exocellulase (TfCel48A) from *Thermobifida fusca*. Appl. Environ. Microbiol. 80 (1), 339–344.

Lee, W.-C., Kuan, W.-C., 2015. Miscanthus as cellulosic biomass for bioethanol production. Biotechnol. J. 10 (6), 840–854.

Li, C., Tanjore, D., He, W., Wong, J., Gardner, J.L., Sale, K.L., Simmons, B.A., Singh, S., 2013. Scale-up and evaluation of high solid ionic liquid pretreatment and enzymatic hydrolysis of switchgrass. Biotechnol. Biofuels 6, 154.

Lu, S., Wang, J., Chitsaz, F., Derbyshire, M.K., Geer, R.C., Gonzales, N.R., Gwadz, M., Hurwitz, D.I., Marchler, G.H., Song, J.S., Thanki, N., Yamashita, R.A., Yang, M., Zhang, D., Zheng, C., Lanczycki, C.J., Marchler-Bauer, A., 2020. CDD/SPARCLE: the conserved domain database in 2020. Nucleic Acids Res. 48 (D1), D265–D268.

Otsuka, M., Ishida, A., Nakayama, Y., Saito, M., Yamazaki, M., Murakami, H., Nakamura, Y., Matsumoto, M., Mamoto, K., Takada, R., 2004. Dietary supplementation with cellooligosaccharide improves growth performance in weanling pigs. Anim. Sci. J. 75 (3), 225–229.

Parisutham, V., Chandran, S.P., Mukhopadhyay, A., Lee, S.K., Keasling, J.D., 2017. Intracellular cellobiose metabolism and its applications in lignocellulose-based biorefineries. Bioresour. Technol. 239, 496–506.

Resch, M.G., Baker, J.O., and Decker, S.R. (2015). Low solids enzymatic saccharification of lignocellulosic biomass laboratory. Natl. Renew. Energy Lab. NREL/TP-5100-63351 1–9.

Roberfroid, M., Slavin, J., 2000. Nondigestible oligosaccharides. Crit. Rev. Food Sci. Nutr. 40 (6), 461–480.

Sanderson, K., 2011. Lignocellulose: A chewy problem. Nature 474 (7352), S12–S14.

Sathitsuksanoh, N., Zhu, Z., Zhang, Y.-H., 2012. Cellulose solvent-based pre-treatment for corn stover and avicel: concentrated phosphoric acid versus ionic liquid [BMIM] Cl. Cellulose 19 (4), 1161–1172.

Schneider, CA, Rasband, WS, Eliceiri, KW, 2012. NIH Image to image J. 25 years of image analysis. Nature Methods 9 (7), 671–675.

Sluiter, A, Hames, B, Hyman, D, Payne, C, Ruiz, R, Scarlata, C, Sluiter, J, Templeton, D, Wolfe, J, 2008. Determination of total solids in biomass and total dissolved solids in liquid process samples, laboratory analytical procedure (LAP). Technical Report NREL/TP-510-42621.

Song, J.M., Hong, S.K., An, Y.J., Kang, M.H., Hong, K.H., Lee, Y.-H., Cha, S.-S., 2017. Genetic and structural characterization of a thermo-tolerant, cold-active, and acidic endo-β-1,4-glucanase from Antarctic springtail, *Cryptopygus antarcticus*. J. Agric. Food Chem. 65 (8), 1630–1640.

Tanghe, M., Danneels, B., Camattari, A., Glieder, A., Vandenberghe, I., Devreese, B., Stals, I., Desmet, T., 2015. Recombinant expression of *Trichoderma reesei* Cel61A in *Pichia pastoris*: optimizing yield and N-terminal processing. Mol. Biotechnol. 57 (11-12), 1010–1017.

Tolonen, L.K., Juvonen, M., Niemelä, K., Mikkelson, A., Tenkanen, M., Sixta, H., 2015. Supercritical water treatment for cello-oligosaccharide production from microcrystalline cellulose. Carbohydr. Res. 401, 16–23.

Watson, B.J., Zhang, H., Longmire, A.G., Moon, Y.H., Hutcheson, S.W., 2009. Processive endoglucanases mediate degradation of cellulose by *Saccharophagus degradans*. J. Bacteriol. 191 (18), 5697–5705.

Wu, S., Wu, S., 2020. Processivity and the mechanisms of processive endoglucanases. Appl. Biochem. Biotechnol. 190 (2), 448–463.

Yang, M., Zhang, K.D., Zhang, P.Y., Zhou, X., Ma, X.Q., Li, F.L., 2016. Synergistic cellulose hydrolysis dominated by a multi-modular processive endoglucanase from *Clostridium cellulosi*. Front. Microbiol. 7, 1–8.

Zhang, Y.-H.-P., Cui, J.-B., Lynd, L.R., Kuang, L.R., 2006. A transition from cellulose swelling to cellulose dissolution by o-phosphoric acid: evidence from enzymatic hydrolysis and supramolecular structure. Biomacromolecules 7, 644–648.

Zhang, Y.-H., Lynd, L.R., 2003. Cellodextrin preparation by mixed-acid hydrolysis and chromatographic separation. Anal. Biochem. 322 (2), 225–232.

Zhu, Z., Sathitsuksanoh, N., Vinzant, T., Schell, D.J., McMillan, J.D., Zhang, Y.-H., 2009. Comparative study of corn stover pretreated by dilute acid and cellulose solvent-based lignocellulose fractionation: Enzymatic hydrolysis, supramolecular structure, and substrate accessibility. Biotechnol. Bioeng. 103 (4), 715–724.

Zverlov, V.V., Schantz, N., Schwarz, W.H., 2005. A major new component in the cellulosome of *Clostridium thermocellum* is a processive endo-β-1,4-glucanase producing cellotetraose. FEMS Microbiol. Lett. 249, 353–358.